COMPDYN 2013
4th ECCOMAS Thematic Conference on
Computational Methods in Structural Dynamics and Earthquake Engineering
M. Papadrakakis, V. Papadopoulos, V. Plevris (eds.)
Kos Island, Greece, 12–14 June 2013

HIGH-SPEED TRAIN PASSAGE EFFECTS IN BUILDINGS: VIBRATION ASSESSMENT AND ISOLATION

A. Romero[1], **M. Solís**[2], **P. Galvín**[3]

Escuela Técnica Superior de Ingeniería. Universidad de Sevilla
Camino de los Descubrimientos s/n, 41092 Sevilla, Spain
e-mail: {aro[1],msolis[2],pedrogalvin[3]}@us.es

Keywords: Dynamic soil-structure interaction, Resonant response, BEM-FEM model, High Speed Train, Isolation system

Abstract. *This paper analyses train induced vibration in buildings. Emission, transmission and immission mechanisms are considered rigorously. Track-ground-building interaction have been studied, concluding that maximum vibration levels are achieved in the floors of the structure. Building induced vibration due to an impulsive load applied at the track have been analysed. The results show an amplification of the structure response around the natural frequencies. Also, an attenuation in the medium-high range frequency is found. Finally, the effects produced by the high speed trains have been investigated. The conclusions show that vibration levels could exceed the limits set by the standards. In theses cases, corrective actions are required. Effectiveness of isolated track systems is evaluated*

1 INTRODUCTION

Induced vibration and radiated noise in buildings due to railway traffic are two of the most important tasks in the design of the new high-speed lines (HSL). This problem (Figure 1) consists of the emission of vibration, wave propagation in soil and the building immission of incident wave field. Vibration levels on attached buildings to HSL depend on the distance to the road, the transmitted load by the train, the train speed, the characteristics of the track and the dynamic properties of the soil. Moreover, structural characteristics of the building and the foundation determine the dynamic response. Taking into account that vibrations produced by train passages may induced high levels, it is necessary to analyse those points on the track where buildings are close and, if necessary, get mitigation actions.

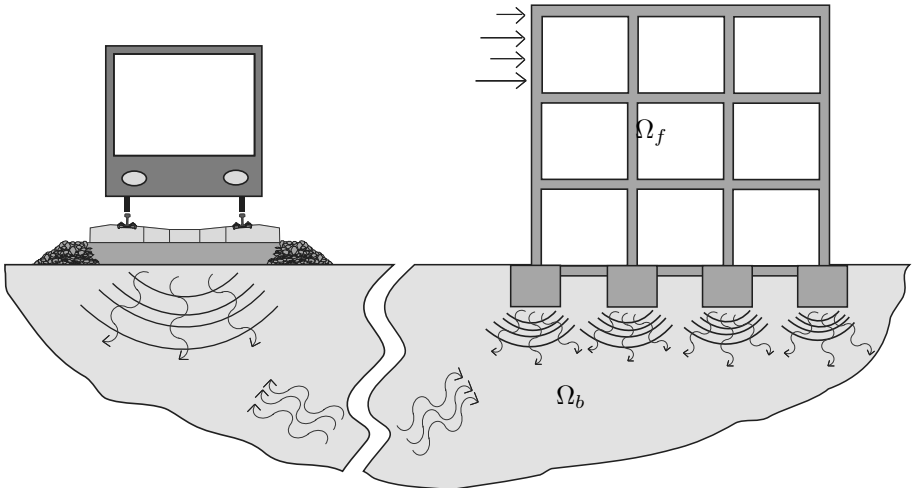

Figure 1: Emission, transmission and immision of train induced vibrations on buildings.

Building vibration analysis requires numerical models which allow to represent adequately generation and propagation mechanisms, as well as the dynamic effects on the structure. Numerical models based on the Boundary Element Method (BEM) and the Finite Element Method (FEM) allow to study soil-structure interaction (SSI) problems rigorously. The BEM [1] is especially suited for the analysis of wave propagation in soils. Sommerfeld radiation condition [2] is satisfied implicitly and the semi-infinite character of soils is well considered. The FEM is very useful to analyse the dynamic behaviour of structures taking into account nonlinear effects [3].

Number of works on the dynamic effects in buildings produced by trains is not very extensive. Numerical models differ in the modelization of the mechanisms involved in this problem, and the formulation can be simplified if some mechanisms are decoupled. Auersch [4, 5, 6] presented a simplified model to predict vibration in buildings. This model allows to take into account the effect of the SSI and the dynamic behaviour of buildings. In these works, Auersch concluded that resonance effects are moderate and decrease at high frequency when SSI is considered.

Simplified models present limitations related to the real geometry of the structure and the building foundation excitation. If these constraints are not acceptable, three dimensional (3D) numerical models are required. Pyl et al. [7, 8] presented one of the first works in which a 3D BEM-FEM model was used. In theses works, the authors analysed the response of a detached house considering that the immission mechanism were decoupled. Similarly, François

et al. [9] presented an analysis of the SSI influence in the road traffic induced vibrations on buildings, and they concluded that the vibration levels depend on the relative stiffness between the foundation and the soil. Fiala et al.[10] analysed the effectiveness of different mitigation system in buildings, using a numerical model developed in two dimensions and a half (2.5D) and based in the substructure method. Mitigation system consisted in the complete or partial isolation room, and also in the use of dampers at the building foundation. Authors concluded that the latter measure was the most effective of those studied.

However, the isolation of buildings using mitigation elements in the structure is limited to the construction of new buildings or the modification of existing ones. Alternatively, isolated railway track systems are studied in this paper. A numerical model has been used to study this problem. The model is formulated in time domain and it is based on the boundary element method and on the finite element method. This model considers the dynamic interaction between vehicle, track, soil and other structures that break the uniformity of the track, such as buildings and underpasses. The proposed model allows to study the actual geometry of the problem and represents the quasi-static and the dynamic excitation mechanisms.

This work was done using SSIFiBo 1.0 MATLAB toolbox for studying Soil-Structure Interaction (SSI) problems in time domain. SSIFiBo is a general purpose package of functions for mechanical and civil engineering research. The package is based on the BEM and FEM elastodynamic formulations in time domain, on the FEM-BEM coupled formulation, and on nonlinear SSI methodology. The SSIFiBo functioning is briefly described in this paper.

2 NUMERICAL MODEL

The boundary element system of equations can be solved step-by-step to obtain the time variation of the boundary unknowns, i.e. displacements and tractions. Piecewise constant time interpolation functions are used for tractions and piecewise linear functions for displacements. The fundamental displacement and traction solutions are evaluated analytically without much difficulty, and nine node rectangular and six node triangular quadratic elements are used for spatial discretization. Explicit expressions of the fundamental displacement and traction solutions corresponding to an impulse point load in a three-dimensional elastic full space can be seen in reference [11]. An approach based on the idea of using a linear combination of equations for several time steps in order to advance one step is used to ensure that the stepping procedure is stable in time. Details of this stabilization approach can be found in [12].

Once the integral equation is discretized one obtains the following equation for each time step:

$$\mathbf{H}^{nn}\mathbf{u}^{n} = \mathbf{G}^{nn}\mathbf{p}^{n} + \sum_{m=1}^{n-1}(\mathbf{G}^{nm}\mathbf{p}^{m} - \mathbf{H}^{nm}\mathbf{u}^{m})\exp\left[-2\pi\alpha(n-m)\Delta t\right] \tag{1}$$

where $\mathbf{u}^{n}$ is the displacement vector and $\mathbf{p}^{n}$ is the traction vector at the end of the time interval n, and $\mathbf{H}^{nn}$ and $\mathbf{G}^{nn}$ are the full unsymmetrical boundary element system matrices, in the time interval n, α is the soil attenuation coefficient and Δt is the time step. The right hand side term derived from previous steps is damped by an exponential coefficient using a linearly increasing exponent with time [13].

Usually, the Spectral Analysis of Surface Waves (SASW) is used to determinate the dynamic soil properties at the studied site. In this test, ground vibrations are generated by means of hammer impacts on a foundations. The response is measured at several points at the soil's surface. The soil's damping coefficient α can be estimated from these measurements solving an inverse problem (a minimization procedure where the variable is α).

The equation which results from the finite element method can be expressed symbolically as follows if an implicit time integration Newmark method is applied [14]:

$$\mathbf{D}^{nn}\mathbf{u}^{n} = \mathbf{f}^{n} + \mathbf{f}^{n-1} \tag{2}$$

where $\mathbf{D}^{nn}$ is the dynamic stiffness matrix, $\mathbf{u}^{n}$ the displacement vector and $\mathbf{f}^{n}$ the equivalent force vector, in the time interval n.

A multi-body model is used to represent the train-track dynamic interaction due to an axle passage [15]. The primary and secondary suspensions isolate the carriages from the track vibrations. The axles and the car body are considered as rigid parts and the primary and secondary suspensions are represented by spring and damper elements [16].

Coupling boundary element and finite element sub-regions entails satisfying equilibrium and compatibility conditions at the interface between both regions.

3 COMPUTATIONAL BACKGROUND

This paper uses the SSIFiBo 1.0 MATLAB toolbox[1] devoloped to study SSI problems in time domain. SSIFiBo is a general purpose package of functions for mechanical and civil engineering research. The package is based on the visco-elastodynamic formulation in time domain proposed by Galvín and Domínguez [11], on the FEM-BEM coupled formulation presented by Galvín et al. [15] to study train induced vibrations, and on the work by Romero et al. [17] for analysing nonlinear SSI problems.

SSIFiBo 1.0 MATLAB toolbox is based on the three dimensional boundary element and finite element formulation in time domain. BEM functions include elemental subdivision and constant velocity approach in order to improve the stability and the accuracy of the method. Computational effort has been reduced with truncation techniques and interpolation procedures. Two different FEM formulations have been used: the nonlinear Newmark GN22 scheme proposed by Chang [18], and the implicit Green's function approach presented by Soares and Mansur [19].

The numerical model allows domain decomposition into subdomains represented by BEM and FEM. Coupling of the equations of the subdomains requires that equilibrium of forces and compatibility of displacements at the interface are satisfied. SSIFiBo 1.0 toolbox includes two different coupling algorithms: a direct coupling procedure, and a nonlinear coupling algorithm to analyse contact effects at the soil-structure interfaces. It is also available a numerical model to study train induced vibrations.

This package has not a FEM preprocessor. Instead of, commercial or freeware FEM distributions are used to made the discretization and to compute mass, damping and stiffness matrices.

FEM and BEM algorithms require large computing resources (CPU and memory storage). The package allows running parallel tasks using several CPUs on a computer. The workload is distributed among the available processors with high performance. The package modularity allows simple and efficient implementation of new enhancements. Therefore, it could be a powerful tool for researching.

4 TRAIN INDUCED VIBRATION ON A THREE STORY BUILDING

This section concerns with the evaluation of building vibrations induced by an AVE S100 High-Speed Train (HST) passage at $v = 300\,\text{km/h}$. The building is located at $20\,\text{m}$ from the track.

[1] http://personal.us.es/pedrogalvin/ssifibo.en.html

The building consists of three floors ($14.4\,\text{m} \times 10.8\,\text{m}$) with height equal to $3\,\text{m}$. Each floor is supported by 8 concrete columns with cross section of $0.3\,\text{m} \times 0.3\,\text{m}$. The structure is reinforced by a concrete core of $0.15\,\text{m}$ thick and was built on a continuous slab with thickness $0.3\,\text{m}$. A damping $\xi = 2\,\%$ is estimated for the structure in the frequency range up to $80\,\text{Hz}$.

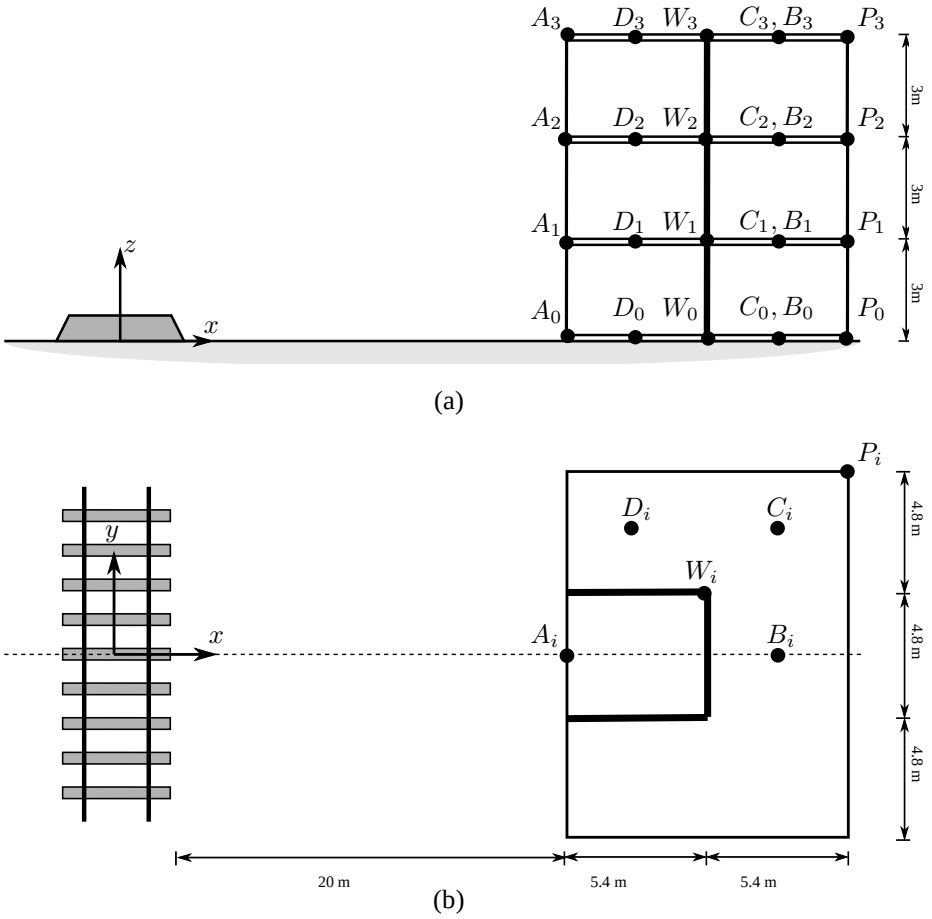

Figure 2: Three story building geometry: (a) frontal and (b) plan view.

The structure was modelled with finite elements. The element size was selected to obtain precise results for a maximum frequency 80 Hz, according to the minimum bending wave wavelengths.

All the track systems considered in this paper are composed of two UIC60 rails with a bending stiffness $E_r I_r = 6.45 \times 10^6$ Nm^2 and a mass per unit length $m_r = 60.3$ kg/m for each rail. The rail-pads are 10 mm thick and their stiffness and damping values are $k_{rp} = 150 \times 10^6$ N/m and $c_{rp} = 13.5 \times 10^3$ Ns/m, respectively. The prestressed concrete monoblock sleepers have a length $l_{sl} = 2.60$ m, a width $w_{sl} = 0.235$ m, a height $h_{sl} = 0.205$ m (under the rail) and a mass $m_{sl} = 300$ kg. A distance $d_{sl} = 0.6$ m between sleepers is considered. The rails and the sleepers are modelled as Bernoulli-Euler beam elements and the rail-pads are modelled as spring-damper elements.

The resilience of the ballast tracks is due to two layers: a ballast layer on a subballast layer. The ballast has a Young's modulus $E_b = 280 \times 10^6$ N/m^2, a shear modulus $G_b = 116 \times 10^6$ N/m^2 and a density $\rho_b = 1500$ kg/m^3. The subballast layer has a Young's modulus $E_{sb} = 140 \times 10^6$ N/m^2, a shear modulus $G_{sb} = 58 \times 10^6$ N/m^2 and a density $\rho_{sb} = 1500$ kg/m^3. The damping value in both layers is $c_b = 24 \times 10^3$ Ns/m^2. The width of the ballast equals 2.92 m and the

height $h_b = 0.7$ m. The ballast and the subballast layers are represented by solid elements.

The slab track systems are composed of a concrete slab on a hydraulic subbase. The concrete slab has a Young's modulus $E_s = 34 \times 10^9$ N/m^2, a shear modulus $G_s = 14.2 \times 10^9$ N/m^2 and a density $\rho_s = 2500$ kg/m^3. The hydraulic subbase has a Young's modulus $E_{hs} = 10 \times 10^9$ N/m^2, a shear modulus $G_{hs} = 4.2 \times 10^9$ N/m^2, a density $\rho_{hs} = 2500$ kg/m^3 and the same width as the concrete slab. The slab and the subbase are represented by solid elements.

In the case of the isolated tracks, a slab mat is considered under the subballast layer (Figure 3.(a)) or the hydraulic subbase (Figure 3.(b)). For a isolated track, the isolation frequency is defined as the resonance frequency of a single-degree-of-freedom system with a mass equal to the track's mass per unit length, m_s, and stiffness equal to the vertical stiffness of the mat bearings, k_f:

$$f_m = \frac{1}{2\pi}\sqrt{\frac{k_f}{m_s}} \tag{3}$$

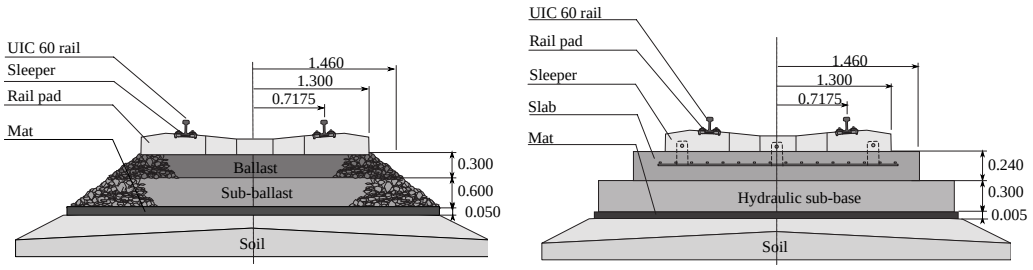

(a) (b)

Figure 3: Isolated track systems: (a) ballast track and (b) slab track.

The tracks are located at the surface of a homogeneous half-space that represents a soft soil, with a S–wave velocity $c_s = 150$ m/s, a P–wave velocity $c_p = 300$ m/s, and density $\rho = 1850$ m/s. These soil properties coincide with those obtained for the upper soil layer from experimental measurements in the HSL between Córdoba and Málaga [20].

Listing 1 shows the SSIFiBo input file, including soil properties, the structural damping, train type and track unevenness.

Figure 4 shows track, soil and structure wave field induced by an impulsive load acting at both rails. Displacements are normalized to soil properties, load amplitude and distance to the point load ($\tilde{u} = \pi c_s^2 \rho u r / p_0$). The incident wave field induced large vertical deformations on the floors.

Next, train induced vibrations by an AVE S100 HST travelling at $v = 300$ km/h are studied. Figure 6 shows the vertical acceleration time histories and frequency contents at the top floor and the ground floor of the structure, considering an unisolated ballast track. Frequency content shows peaks at bogie passage frequency, $f_b = 4.41$ Hz, and at the building resonance frequencies. A clear amplification between both floors is detected. Also, medium range frequency due to the dynamic contribution can be observed.

Figure 6 shows the running RMS value and the one-third octave band spectra of the vertical acceleration at ground floor and third floor. Again, clear amplification can be observed at the third floor response regarding to the ground floor. One-third octave band spectra shows local maximum at frequency bands related with the bogie passing frequency ($f_b = 4.41$ Hz) and building resonance frequencies close to 20 Hz.

```
% JOB TITLE
JOB='EXAMPLE3'

% SOIL PROPERTIES
CP=300          % P-wave propagation velocity [m/s]
CS=150          % S-wave propagation velocity [m/s]
RO=1850         % Density [kg/m^3]
DAMP=0.09       % Damping

% STRUCTURAL DAMPING (C=alpha*M+beta*K)
ALPHA=2.35      % [s^-1]
BETA=1.18e-4    % [s]

% TIME STEP OPTIONS
NSTEP=173       % Number of time steps
AT=0.006        % Time interval [s]

% TRAIN AND TRACK PROPERTIES
TRAIN='S100'    % Train type
SPEED=83        % Train speed [m/s]
UNEVENNESS='A'  % ISO 8608 road classification (range from 'A' to 'H')

% CALL SSIFIBO
ssifibo(JOB,CP,CS,RO,DAMP,ALPHA,BETA,NSTEP,AT,TRAIN,SPEED,UNEVENNESS)
```

Listing 1: Input file to compute train induced vibration on a three story building.

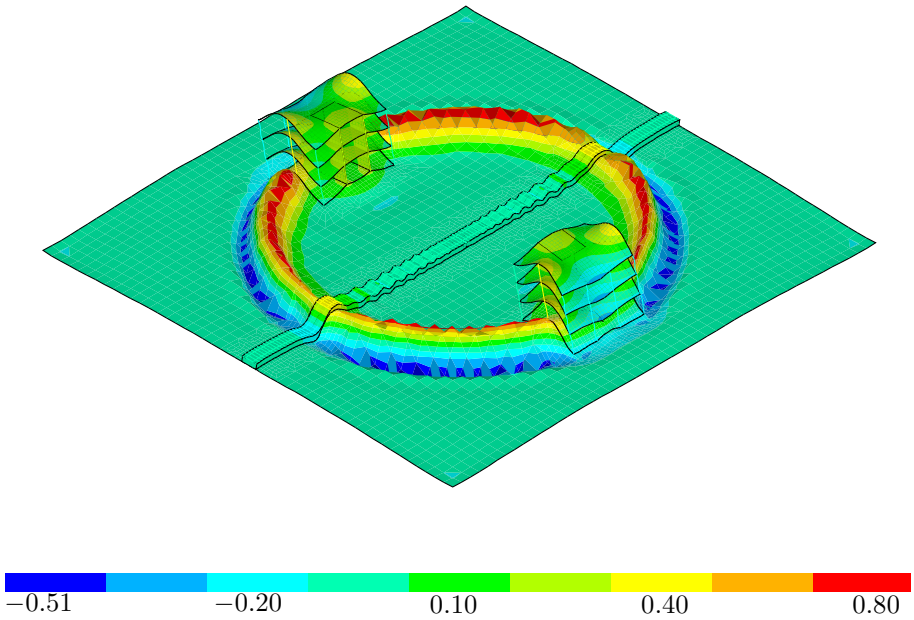

Figure 4: Dimensionless wave field due to an impulsive load acting at the track.

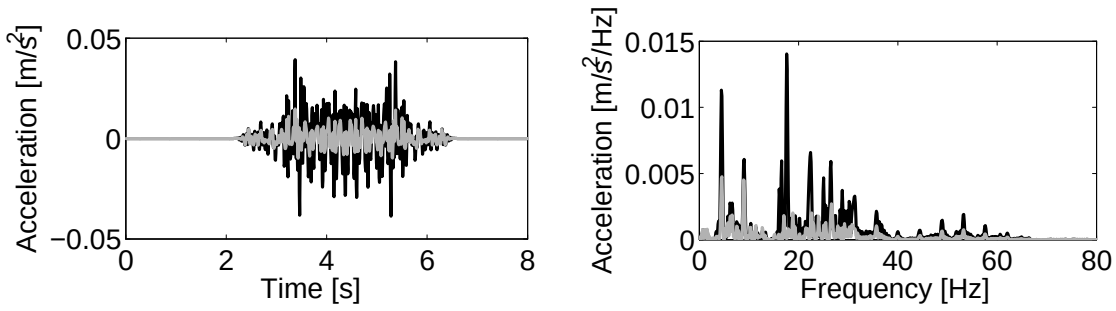

(a) (b)

Figure 5: (a) Time history and (b) frequency content of vertical acceleration at the ground floor (grey line) and the top floor (black line), during the passage of an AVE S100 HST at a speed $v = 300$ km/h.

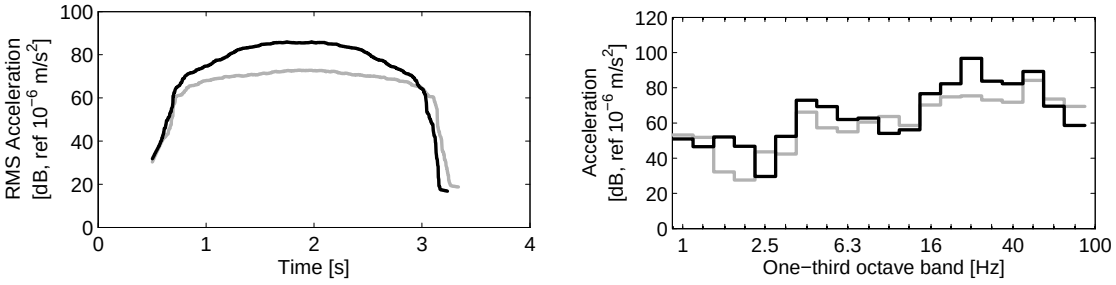

(a) (b)

Figure 6: (a) Running RMS value and (b) one-third octave band spectra of the vertical acceleration at ground floor (grey line) and third floor (black line) during the passage of an AVE S100 HST at a speed $v = 300$ km/h.

5 VIBRATION ASSESSMENT AND ISOLATION

In this section, the assessment of track isolation is evaluated. That solution gives a effective control of ground borne vibration after the cut-off track isolation frequency f_0. However,

response amplification occurs around the track isolation frequency f_m. Efficiency of isolated track systems depends on insertion loss, IL, and cut off frequency of the mat [21]. In this work, two different mats are studied. Table 1 shows the track isolation frequency f_m and the cut-off frequency f_0 for the isolated ballast and slab track.

Track system	E_m [N/m^2]	ρ_m [kg/m^3]	ζ_m [-]	f_m [Hz]	f_0 [Hz]
Isolated ballast track I	0.26×10^6	100	0.1	8.8	12.4
Isolated ballast track II	2.15×10^6	100	0.3	23.8	33.0
Floating slab track I	0.26×10^6	100	0.1	8.9	12.5
Floating slab track II	2.15×10^6	100	0.3	25.1	36.4

Table 1: Properties of isolated track systems: mat Young's modulus (E_m), density (ρ_m) and damping (ζ_m); isolation (f_m) and cut off (f_0) frequencies.

Figure 7 presents the ground borne vibration for a point located at $28\,\text{m}$ from the track, due to an impulsive load $p(t) = p_0 H(t - 0.025\,\text{s})$ acting in both rails. Results show an amplification around the isolation track frequency f_m and a mitigation for higher frequencies. Maximum isolation is reached for floating slab track when soft mat is used and for frequencies above $10\,\text{Hz}$.

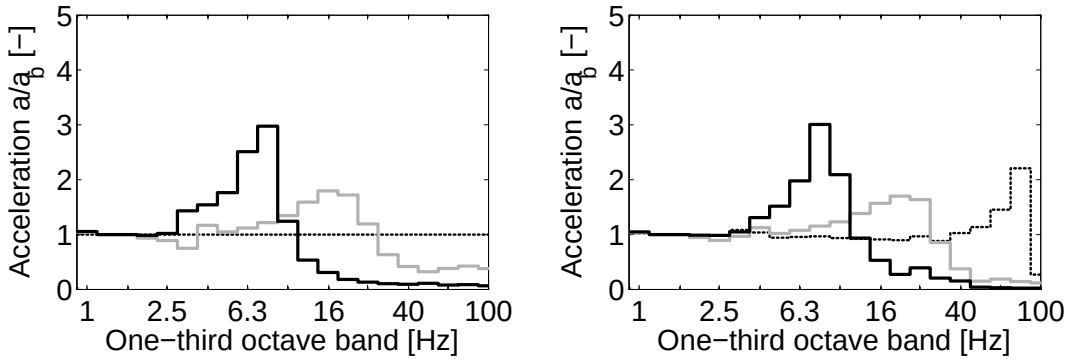

(a) Ballast track. (b) Slab track.

Figure 7: Ground borne amplification at a point located at $28.1\,\text{m}$ from the track due to impulsive load acting at the rails, considering unisolated track system (dotted black line), isolated system I (solid black line) and isolated system II (solid grey line).

Having examined the response at the free field, building response due to the incident wave field is presented in Figure 8. There is an amplification around the resonant frequency of the track, that is close to the natural frequencies of the structure. After, building response is mitigated and a maximum isolation level is reached for a ballast track with soft mat for frequencies above $25\,\text{Hz}$. Unisolated slab track does not allow an effectiveness ground borne vibration control, as can be seen in Figure 7.(b). That figure shows an amplification at high frequency. However, this effect occurs for frequencies higher than building resonant frequencies and does not affect to the structure response (Figure 8.(b)).

Finally, Figures 9 and 10 show running RMS value and the insertion loss of the vertical acceleration at the third floor, for a HST passage at $v = 300\,\text{km/h}$ travelling on the different tracks. The insertion loss is obtained from the relation between the vibration levels for unisolated ballas track, a_b, and the others track systems:

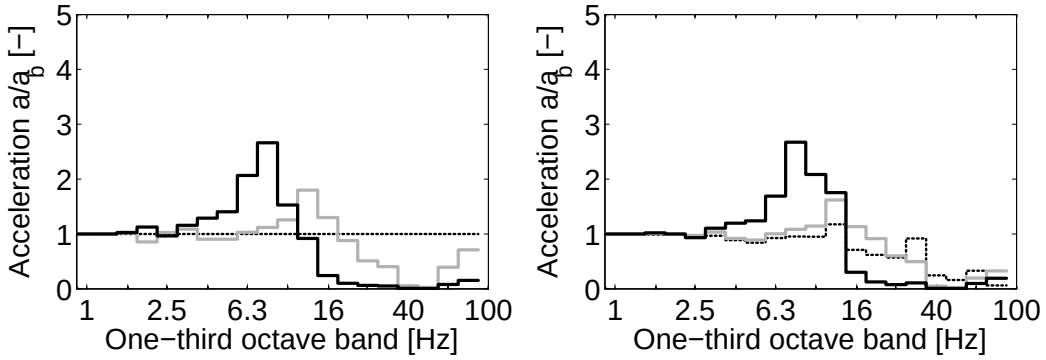

(a) Ballas track. (b) Slab track.

Figure 8: Building amplification at the top floor due to impulsive load acting at the rails, considering unisolated track system (dotted black line), isolated system I (solid black line) and isolated system II (solid grey line).

$$IL = 20 \log_{10} \left(\frac{a}{a_b} \right) \tag{4}$$

Isolated ballast tracks exhibit a maximum mitigation of $9\,$dB and an insertion loss of $-35\,$dB. Floating slab tracks produce an increase of the running RMS value of $2.5\,$dB and a decrease of $-29\,$dB. Both track systems induced an amplification around the track resonant frequency.

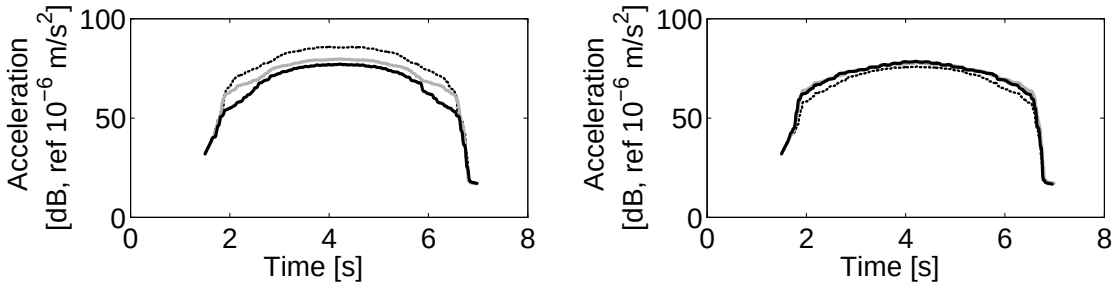

(a) Ballast track. (b) Slab track.

Figure 9: Running RMS value of the vertical acceleration at the top floor during the passage of an AVE S100 HST at a speed $v = 300\,$km/h, considering unisolated track system (dotted black line), isolated system I (solid black line) and isolated system II (solid grey line).

6 CONCLUSIONS

In this paper, HST induced vibration in buildings has been presented. A numerical model based on time domain three-dimensional finite element and boundary element formulations was used. This model allows to take into account local soil discontinuities, underground constructions, and nearby structures that break the uniformity of the geometry along the track line. Track and other structures are modelled using the finite element method and their non-linear behaviour could be considered because a time domain formulation is employed. The soil was represented using the boundary element method, where a full space fundamental solution was used in combination with quadratic boundary elements. The train vehicle was modelled as a multi-body and, therefore, the quasi-static and the dynamic excitation mechanisms can be considered, taking into account the dynamic effects due to discrete sleeper support and the wheel and rail irregularities.

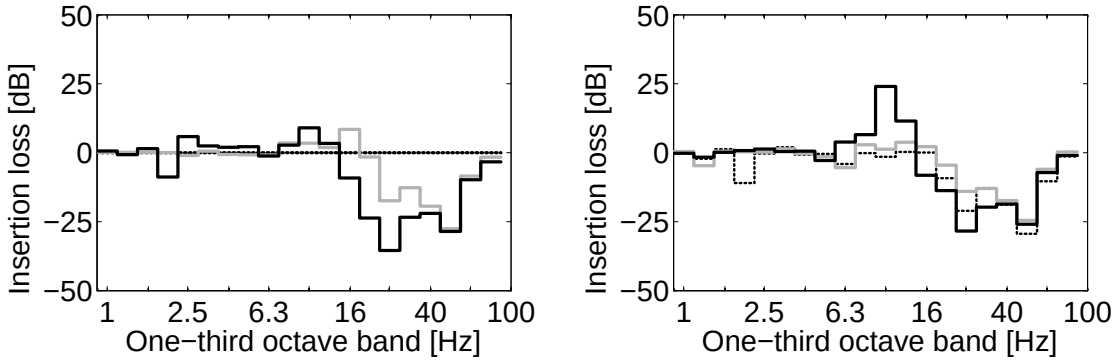

(a) Ballast track.

(b) Slab track.

Figure 10: Insertion loss of the vertical acceleration at the top floor during the passage of an AVE S100 HST at a speed $v = 300$ km/h, considering unisolated track system (dotted black line), isolated system I (solid black line) and isolated system II (solid grey line).

Results show that induced vibrations by HST are amplified around building resonance frequencies. Efficiency of isolation mats has been evaluated. Choice of mats characteristics are related to track properties, soil behaviour and building resonance frequencies. Building response could be amplified if the isolation frequency is close to the natural frequencies of the structure. Ballasted track with low stiffness mat allows to reduce vibration levels and, therefore, that system becomes an effective and alternative system to floating slab tracks.

7 ACKNOWLEDGEMENT

This research was funded by the Spanish Ministry of Economy and Competitiveness (Ministerio de Economía y Competitividad) through research project BIA2010-14843. Financial support is gratefully acknowledged. The authors also wish to acknowledge the support provided by the Andalusian Scientific Computing Centre (CICA)

REFERENCES

[1] J. Domínguez. *Boundary elements in dynamics*. Computational Mechanics Publications and Elsevier Aplied Science, Southampton, 1993.

[2] A.C. Eringen and E.S. Suhubi. *Elastodynamics, Volume 2, Linear theory*. Academic Press, New York, USA, 1975.

[3] O.C. Zienkiewicz. *The finite element method*. McGraw-Hill, third edition, 1986.

[4] L. Auersch. Simplified methods for waves propagation and soil-structure interaction: The dispersion of layered soil and the aproximation of FEBEM results. *Procedings of 6th International Conference on Structural Dynamics (EURODYN 2005), Millpress, Rotterdam*, pages 101–112, 2005.

[5] L. Auersch. Two- and three-dimensional methods for the assessment of ballast mats, ballast plates and other isolators of railway vibrations. *International Journal of Acoustics and Vibration*, 11(3):167–176, 2006.

[6] L. Auersch. Building response due to ground vibration – Simple prediction model based on experience with detailed model and measurements. *International Journal of Acoustics and Vibration*, 15(3):101–112, 2010.

[7] L. Pyl, G. Degrande, and D. Clouteau. Validation of a source–receiver model for road traffic induced vibrations in buildings. II: Receiver model. *Journal of Engineering Mechanics, Procedings of the ASCE*, 130(12):1394–1406, 2004.

[8] L. Pyl, G. Degrande, G. Lombaert, and W. Haegeman. Validation of a source–receiver model for road traffic induced vibrations in buildings. I: Source model. *Journal of Engineering Mechanics, Procedings of the ASCE*, 130(12):1377–1393, 2004.

[9] S. François, L. Pyl, H.R. Masoumi, and G. Degrande. The influence of dynamic soil–structure interaction on traffic induced vibrations in buildings. *Soil Dynamics and Earthquake Engineering*, 31416(27):655–674, 2007.

[10] P. Fiala, G. Degrande, and F. Augusztinovicz. Numerical modelling of ground-borne noise and vibration in buildings due to surface rail traffic. *Journal of Sound and Vibration*, 301(31416):718–738, 2007.

[11] P. Galvín and J. Domínguez. Analysis of ground motion due to moving surface loads induced by high-speed trains. *Engineering Analysis with Boundary Elements*, 31(11):931–941, 2007.

[12] M. Marrero and J. Domínguez. Numerical behavior of time domain BEM for three-dimensional transient elastodynamic problems. *Engineering Analysis with Boundary Elements*, 27(1):39–48, 2003.

[13] P. Galvín and J. Domínguez. High-speed train-induced ground motion and interaction with structures. *Journal of Sound and Vibration*, 307(3-5):755–777, 2007.

[14] N.M. Newmark. A method of computation for structural dynamics. *ASCE Journal of the Engineering Mechanics Division*, 85(1):67–94, 1959.

[15] P. Galvín, A. Romero, and J. Domínguez. Fully three-dimensional analysis of high-speed train-track-soil-structure dynamic interaction. *Journal of Sound and Vibration*, 329(24):5147–5163, 2010.

[16] X. Sheng, C.J.C. Jones, and D.J. Thompson. A theoretical model for ground vibration from trains generated by vertical track irregularities. *Journal of Sound and Vibration*, 272(3-5):937–965, 2004.

[17] A. Romero, P. Galvín, and J. Domínguez. 3D non-linear time domain FEM-BEM approach to soil-structure interaction problems. *Engineering Analysis with Boundary Elements*, DOI: 10.1016/j.enganabound.2013.01.001, 2012.

[18] S.Y. Chang. Nonlinear error propagation analysis for explicit pseudodynamics algorithm. *Journal of Engineering Mechanics ASCE*, 123:841–850, 2003.

[19] D. Soares and W.J. Mansur. A time domain FEM approach based on implicit Green's functions for non-linear dynamic analysis. *International Journal for Numerical Methods in Engineering*, 62(5):664–681, 2005.

[20] P. Galvín and J. Domínguez. Experimental and numerical analyses of vibrations induced by high-speed trains on the Córdoba-Málaga line. *Soil Dynamics and Earthquake Engineering*, 29(4):641–657, 2009.

[21] R. G. Wettschureck. Measures to reduce structure-borne noise emissions induced by above-ground, open railway lines. *Rail Engineering International*, 31416(2):12–16, 1997.